ELSEVIER

Polymer 42 (2001) 5005–5012

polymer

www.elsevier.nl/locate/polymer

Electrorheological characteristics of phosphate cellulose-based suspensions

S.G. Kim[a], J.W. Kim[a], W.H. Jang[a], H.J. Choi[a,*], M.S. Jhon[b]

[a]*Department of Polymer Science and Engineering, Inha University, Inchon 402-751, South Korea*
[b]*Department of Chemical Engineering, Carnegie Mellon University, Pittsburgh, PA 15213, USA*

Received 22 May 2000; received in revised form 20 November 2000; accepted 27 November 2000

Abstract

As a potential candidate for the development of anhydrous electrorheological (ER) materials, phosphate cellulose particles were synthesized from a phosphoric ester reaction between cellulose particles and a 2 M phosphoric acid–urea mixture, and then dispersed in silicone oil to prepare the phosphate cellulose-based ER fluid. Rheological measurements were carried out via a rotational rheometer with a high voltage generator in both steady and oscillatory shear modes to investigate the effects of electric field strength and particle concentration on ER performance. The results show not only that the ER properties are enhanced by increasing the particle concentration and electric field strength, but also the cellulose-based ER fluids exhibit viscoelastic behavior under an applied electric field due to the chain formation induced by electric polarization between particles. © 2001 Published by Elsevier Science Ltd.

Keywords: Cellulose; Suspension; Electrorheological fluid

1. Introduction

Electrorheological (ER) fluids composed of a suspension of micron-sized particles in a non-conducting fluid form fibrillated particle structures, which are caused by the dielectric constant mismatch of the particles and the insulating oil, in strong electric fields [1,2]. Thus, it is quite natural that dielectric polarization theory appeared, because ER behavior was closely related to dielectric phenomena, and among various polarizations, interfacial polarization is assumed to be responsible for ER phenomena [3,4]. To overcome the shortcomings (thermal instability and corrosion) that wet-base systems [1] possess, various dry-base systems have been investigated with anhydrous particles, including zeolite [5,6], PZT [7], carbonaceous particle [8], and intrinsically polarizable semi-conducting polymers. Special attention has been paid to the polymer-based ER materials. Examples include: acene quinone radical polymers [9,10], polyaniline [11–14], copolyaniline [15–17], polyphenylenediamine [18], polyurethane [19] and polymer–clay nanocomposites with styrene acrylonitrile copolymer [20,21] or polyaniline [22,23].

These materials possess either branched polar groups such as amine ($-NH_2$), hydroxy (–OH) and amino-cyano (–NHCN), or semi-conducting repeated groups. The polar groups may affect the ER behavior by playing the role of the electronic donor under the imposed electric field. The chemical structure of the organic materials is, therefore, an important factor in the ER performance.

The difference between the dry-base and the wet-base systems is the carrier species for particle polarization. The particle chain structure is formed by the migration of ions in the absorbed water in the wet-base ER fluids, whereas the electrons move inside the molecules of the particles in the dry-base ER fluids.

In this paper, we investigate phosphate cellulose as a potential candidate for anhydrous particles in high performance dry-base systems by examining the effect of particle concentration and electric field strength via both steady and oscillatory shear tests. Phosphate cellulose particles are of considerable interest due to their inherent flame resistance and ion-exchange capability [24]. In contrast to a wet-base microcrystalline cellulose ER material with a small amount of adsorbed water [25,26], ER behavior for anhydrous phosphate cellulose suspensions has been recently observed [27,28]. Therefore, the unique feature of the phosphate cellulose-based ER fluid is a dry-base system, possessing similar yield stress compared to other high performance ER fluid such as polyaniline system [29].

To understand the roles of both conductivity and dielectric constant in phosphate cellulose particle-based ER

* Corresponding author. Tel.: +82-32-860-7486; fax: +82-32-865-5178.
E-mail address: hjchoi@inha.ac.kr (H.J. Choi).

0032-3861/01/$ - see front matter © 2001 Published by Elsevier Science Ltd.
PII: S0032-3861(00)00887-9

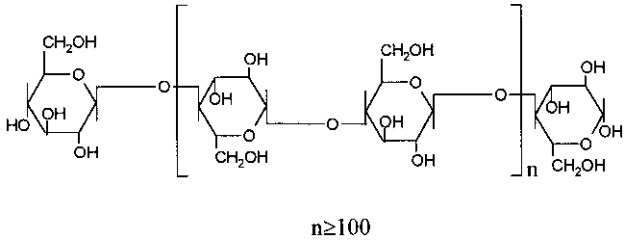

Fig. 1. Structural formula of cellulose.

systems, we examined rheological properties including yield stress of the ER fluids as well as electrical properties such as dielectric constant and conductivity of particles, as a function of phosphoric acid reaction concentration [28]. An ER system with phosphate cellulose particles formed in a 2 M phosphoric acid solution exhibits the highest yield stress (ER performance) compared to the other systems from rheological measurements in both controlled shear rate (CSR) and controlled shear stress modes (CSS).

2. Experimental

Phosphate cellulose particles were synthesized by an esterification of cellulose with an orthophosphoric acid–urea mixture (phosphorylation of cellulose) at room temperature, using the method suggested by Arslanov et al. [30]. Cellulose is a linear syndiotactic homopolymer composed of D-anhydroglucopyranose units, which are linked together by β-(1 → 4)-glycosidic bonds. The molecular structure of cellulose is given in Fig. 1.

At first, aqueous solutions of phosphoric acid (orthophosphoric acid, 85% assay, Junsei Chemical Co., Tokyo, Japan) containing 4 M urea with 2 M phosphoric acid concentrations, which is the optimum molar concentration [28], were prepared by stirring the solutions for 1 h. The

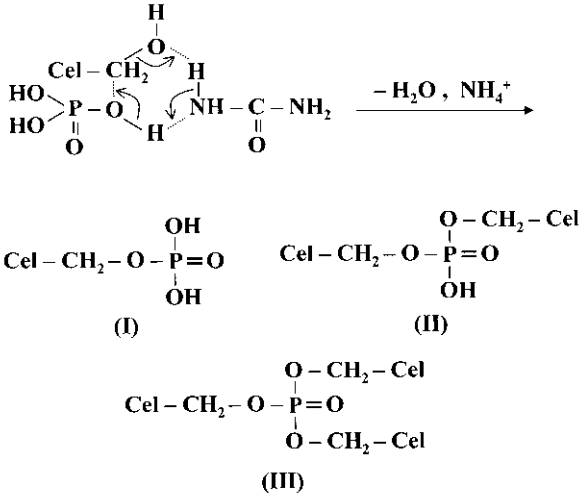

Fig. 2. The phosphoric ester reaction of cellulose.

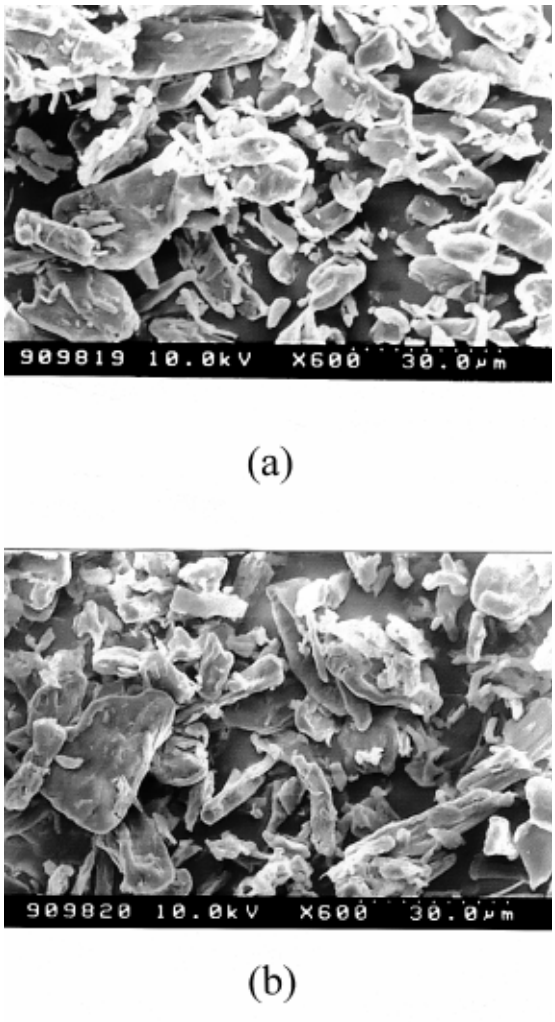

Fig. 3. SEM photographs of: (a) raw cellulose particles, and (b) phosphate cellulose particles.

40 g of raw cellulose particles, with an average size of 20 μm (Sigmacell, Type 20, Sigma Chemical Co., St Louis, USA), were added to 400 cm^3 of phosphoric acid solution with 4 M urea and then stirred for 48 h to allow the phosphoric ester reaction of cellulose.

It was claimed that orthophosphoric acid can form non-crosslinked monosubstituted, crosslinked disubstituted and crosslinked trisubstituted esters with cellulose [30] as shown in Fig. 2. The products obtained are insoluble due to cross-linking. Therefore, they are often characterized by their phosphorus content only. Instead of directly characterizing phosphorous content, the proton (H) content of the phosphate cellulose particles was determined from elemental analysis [28]. The amount of H decreased with the concentration of phosphoric acid solution, indicating that the cellulose hydroxyl groups were esterified with increased concentration of phosphoric acid solution.

After the reaction, the phosphate cellulose particles were washed five times with distilled water to remove any unreacted urea and phosphoric acid remaining on the

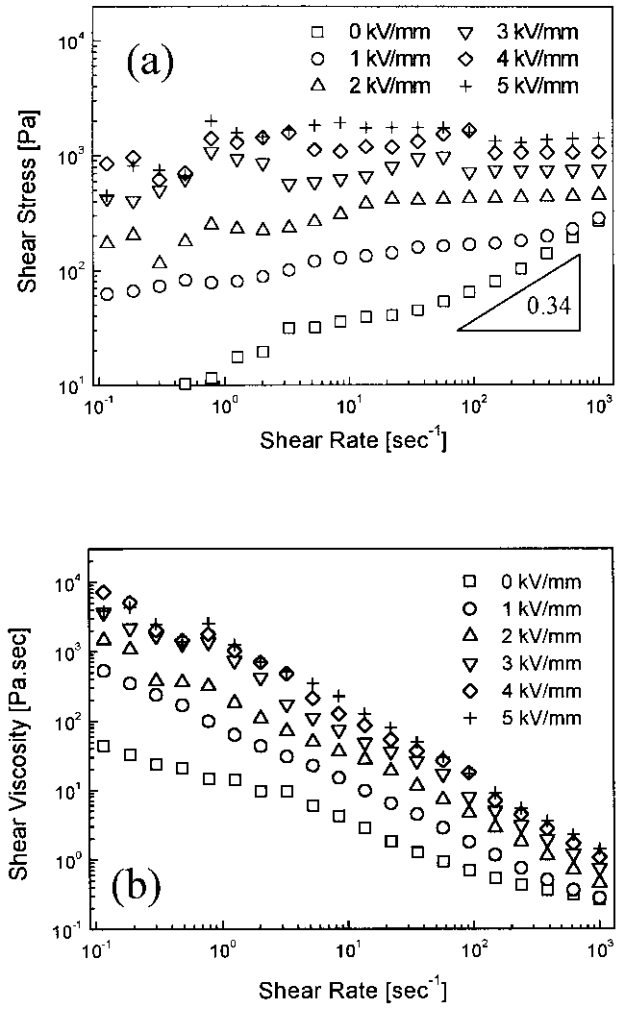

Fig. 4. (a) Shear stress and (b) shear viscosity versus shear rate measured from the CSR mode for 20 vol% phosphate cellulose in silicone oil at six different electric field strengths.

surface of the phosphate cellulose particles and were then filtered using an aspirator. After drying in a vacuum oven for three days (to completely remove water), the dried phosphate cellulose particles were ground using a mixer and then passed through a 38 μm sieve shaker to control the particle size distribution. The density of the phosphate cellulose particles measured via a pycnometer was 1.28 g/cm^3. Note that the density of the phosphate cellulose particles increased linearly with phosphoric acid concentration in the phosphoric ester reaction of cellulose, since a decrease in phosphate particle mass was observed along with a simultaneous increase in phosphoric acid concentration [28].

ER fluids were prepared by dispersing the phosphate cellulose particles in silicone oil (density; 0.956 g/cm^3, kinematic viscosity; 50 cSt), which was dried in a vacuum oven and stored with molecular sieves before use. The prepared ER fluids were stored in a desiccator prior to use and redispersed before every measurement.

The rheological properties of the ER fluids were examined via a system consisting of a rotational Physica rheometer (MC 120, Germany) equipped with a Couette-type geometry, a high-voltage generator (HVG 5000, Germany), and an oil bath for temperature control. To start a run, an ER fluid is placed between a bob and a cup of the measuring geometry (Z3-DIN) with a gap of 1.06 mm, and a DC voltage is applied to the cup. The electric field was applied for 3 min to obtain equilibrium chain-like or columnar structures before applying the shear.

3. Results and discussion

Fig. 3(a) and (b) presents SEM photographs of raw cellulose and phosphate cellulose particles, respectively. The particle shape is rod-like and irregular. In addition, a change in particle shape due to the phosphoric ester reaction of cellulose is hardly detected.

Fig. 4(a) shows the flow behavior of the phosphate cellulose-based ER fluid [particle concentration: 20% (v/v)] obtained in CSR mode at six different applied electric fields. At this high particle volume fraction, the ER fluid exhibits non-Newtonian characteristics even at zero electric field strength by showing a non-linear constitutive relationship between the shear stress (τ) and shear rate ($\dot{\gamma}$), in which the shear rate is defined as $\dot{\gamma} = 2b^2\omega/(b^2 - a^2)$ with ω being the angular velocity of the rotating cylinder and b and a, the radii of the outer and inner cylinder [31].

For $\dot{\gamma} > 1\ \mathrm{s}^{-1}$, $\tau \propto (\dot{\gamma})^n$ with $n = 0.34$, exhibiting shear thinning behavior since the apparent viscosity $\eta \equiv \tau/\dot{\gamma} \propto \dot{\gamma}^{n-1} = \dot{\gamma}^{-0.66}$, decreases with increasing $\dot{\gamma}$. This non-Newtonian shear thinning behavior has been observed also for various suspension systems including magnetic particles [32–34] and silica suspensions [35]. When an electric field was applied to this suspension, τ (or η), which is a function of the $\dot{\gamma}$, abruptly increased over the entire shear rate range, and yield stresses appeared as in a Bingham fluid. Even when an electric field strength of only $E = 1$ kV/mm is applied to the sample, τ is approximately 10 times higher than at zero electric field strength in the low shear rate region ($\dot{\gamma} < 1\ \mathrm{s}^{-1}$).

In our previous study [36], polyaniline-based ER fluids showed that the shear stress behaves in this manner without an applied electric field for $\dot{\gamma} > 40\ \mathrm{s}^{-1}$. This is probably due to an interparticle interaction force indicating that the presence of the electrostatic field affect flow properties in such a high shear rate regime at $E = 1$ kV/mm. In other words, at $\dot{\gamma} > 40\ \mathrm{s}^{-1}$, the shear force dominates the electrostatic interaction among the suspending polyaniline particles.

However, in Fig. 4, the shear stress exhibits a plateau region over the entire range of $\dot{\gamma}$ (including $\dot{\gamma} > 40\ \mathrm{s}^{-1}$). This plateau region becomes broader with the increasing electric field strength. This is probably due to an interparticle interaction force indicating that the presence of the electrostatic field affects flow properties in such a high shear rate regime at $E = 1$ kV/mm. In the case of phosphate

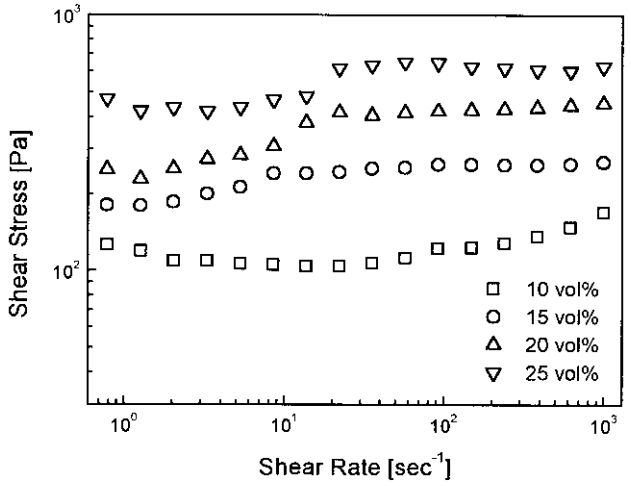

Fig. 5. Shear stress versus shear rate measured from the CSR mode for phosphate cellulose in silicone oil at four different particle concentrations and an electric field strength of 2 kV/mm.

cellulose-based ER fluid, contrary to the polyaniline-based ER fluid, the electrostatic interaction among the suspending phosphate cellulose particles still dominates the shear force at $\dot{\gamma} > 40\ s^{-1}$. This means that the chain-like structure was not fully broken even in the high shear rate regime ($\dot{\gamma} > 40\ s^{-1}$).

In general, the structure in a concentrated suspension can be sufficiently rigid such that it permits the material to sustain a certain level of deforming stress without flowing. The maximum stress that can be sustained without flow is called "the yield stress." For a simple shear flow, this type of behavior is described by the following Bingham model [37]:

$$\begin{aligned} \tau(\dot{\gamma}, E) &= \eta_{pl}(E)\dot{\gamma} + \tau_d(E) \quad \text{if } \tau > \tau_d \\ \dot{\gamma} &= 0 \qquad\qquad\qquad\quad \text{if } \tau < \tau_d \end{aligned} \tag{1}$$

Here, $\tau(\dot{\gamma}, E)$ is the shear stress, τ_d the dynamic yield stress, E the applied electric field strength and η_{pl} the plastic viscosity, which is independent of electric field strength i.e. approximately equal to the high shear rate suspension viscosity in the absence of an electric field [38]. Thus the Bingham model is specified by two material constants τ_d and η_{pl}.

It is generally reported that the apparent shear viscosity, defined as $\eta \equiv \tau/\dot{\gamma}$, which is distinguished from η_{pl} defined in Eq. (1). In addition, it should be noted that the Bingham fluid exhibits the plug-flow behavior at relatively low shear rates. In the Couette cell with a rotating coaxial inner cylinder, flow occurs when $\tau > \tau_d$ in the case of $\tau_b > \tau_d > \tau_a$, in which the radius of the inner cylinder is a, and that of the outer cylinder is b, and the value of shear stress, τ at $r = a$ and $r = b$ are τ_a and τ_b, respectively. Therefore, flow occurs when r is less that a critical value r_c while no flow occurs when r is larger than r_c. This corresponds to plug flow in capillary flow [31].

This Bingham plastic/fluid behavior arises from the columnar structures of the phosphate cellulose particles formed by induced electrostatic interaction between particles. The interaction force stems from the induced dipole moment caused by the interfacial polarization between the conductive dispersed phase and the non-conducting medium [39].

Fig. 4(b) shows that η for the same ER fluid measured at different electric field strengths, displaying a shear thinning behavior. Similar shear thinning behavior has been observed for various ER systems such as polyaniline [12], alumina particle [38], zeolite [5], mesoporous MCM-41 particle [40] and copolyaniline [41].

Flow curves for the phosphate cellulose ER fluid with different particle concentrations at 2 kV/mm are shown in Fig. 5. Shear stresses increase with increasing of the particle concentration over the entire shear rate range. This behavior is similar to that shown in Fig. 4(a).

Fig. 6(a) presents the dependence of static yield stress (τ_y) on electric field strength for various volume fractions of phosphate cellulose-based ER fluid from the CSS mode. In the CSS mode, the ER fluid was stressed by an applied mechanical torque until the particle chain

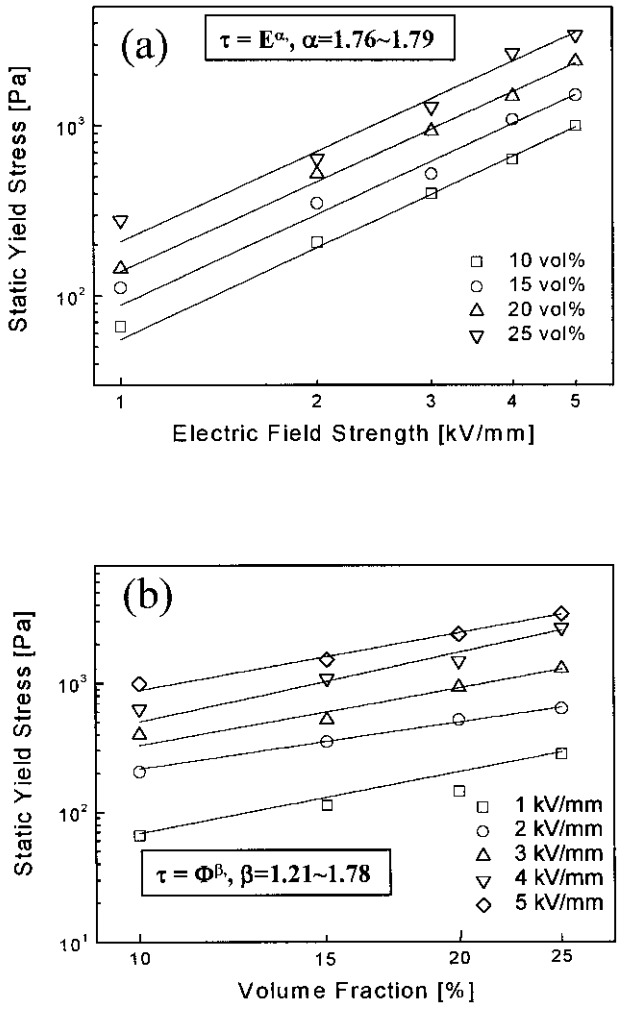

Fig. 6. Static yield stress versus electric field strength (a) and volume fraction (b) from the CSR mode for phosphate cellulose in silicone oil.

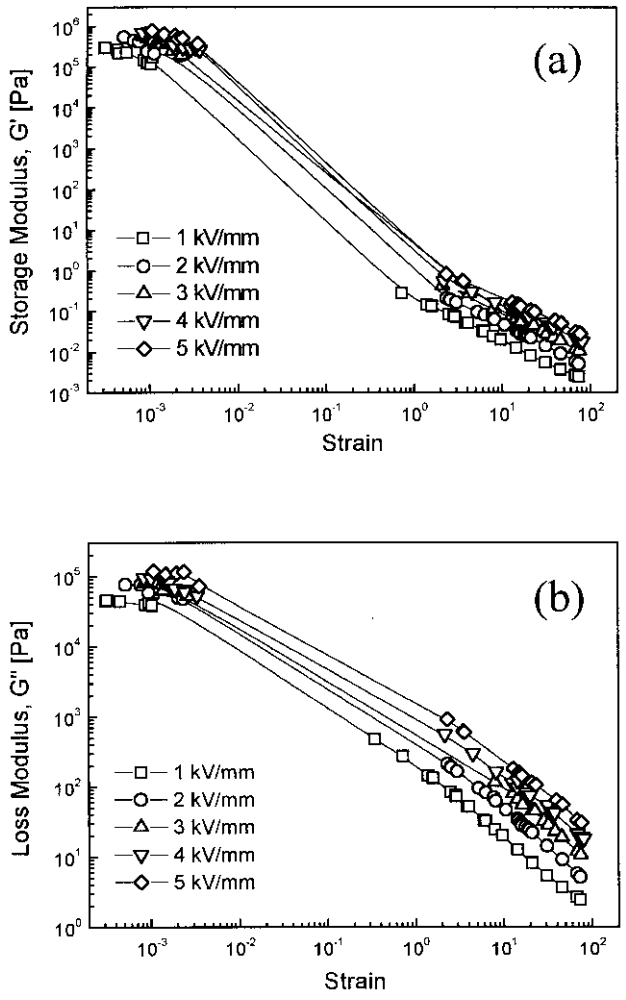

Fig. 7. (a) G' and (b) G'' as a function of static amplitude for 20 vol% phosphate cellulose in silicone oil at five different electric field strengths and a frequency of 1 Hz.

structure was broken to generate flow, and the stress at the onset of flow was static yield stress. Fig. 6(b) shows the effect of phosphate cellulose volume percent on τ_y via the CSS mode. Similar to many other ER fluids, the phosphate cellulose/silicone oil ER system also possesses the property that yield stress increases as both particle concentration and electric field strength increase as a result of an increase in the polarization forces between particles. When the particle concentration is extremely small, there are only a few particle chains or fibrils, and there is only a minute increase in the τ_y.

We proposed a power law relationship between τ_y and the electric field strength (E) or the particle volume fraction (Φ) [42,43]:

$$\tau_y \propto E^{\alpha} \text{ and } \tau_y \propto \Phi^{\beta} \quad (2)$$

The α values in Eq. (2) for phosphate cellulose ER fluid were 1.76–1.79 and Eq. (2) is just approximate because of the change of β with E. The results in this paper differ slightly from the statement that the yield stress is proportional to the square of the electric field strength obtained from the polarization model [44].

In the polarization model, the applied electric field induces electrostatic polarization interactions among the particles and between the particles and the electrodes. Klingenberg et al. [44] studied the electrostatic interaction between the particles using the point dipole limit. Each sphere (or particle) is treated as a dipole only, located at the sphere center and aligned with the applied electric field, with the magnitude of the dipole being given by that induced on an isolated dielectric sphere in a uniform electric field. The net force on each sphere is given by the pairwise summation of the interactions with all of the spheres. Therefore, the polarization model with the point dipole approximation is for a simpler system compared to our phosphate cellulose ER system. The shape of our phosphate cellulose particles was very irregular and rod-like, and a quite broad particle size distribution was also observed (through SEM). Thus, the dipole moment of the particles is not uniform and it may have given the observed $\alpha < 2$.

On the other hand, note that Davis [45] incorporated a nonlinear conductivity effect with the bulk conducting particle model and constructed an alternative yield stress model, showing that "α" approaches 3/2 for high electric field strengths. Ginder et al. [46] also derived τ_y for the field saturation regime via an analytic conductivity based on surface conducting particles and found α becomes 2 at low fields, and α approaches 1.12 at high fields. The applied electric field in this study is considered to be relatively high. This might be also related to our observation $\alpha < 2$. Furthermore, the yield stress of the phosphate cellulose ER fluid is also assumed to be proportional to Φ^{β}. The β values in Eq. (2) were 1.21–1.78. Note that β is strongly dependent on the electric field strength. Eq. (2) indicates that the yield stress is strongly affected by both the electric field strength and the particle concentration.

Dynamic tests by an oscillatory shear were performed and used to study the viscoelastic properties of the solidified ER fluid under applied electric field strength. The results of the strain sweep, which is a sinusoidal amplitude at a constant frequency, are shown in Figs. 7 and 8. At first, these measurements were conducted to determine the linear viscoelastic region of strain from the strain sweep experiment. From Figs. 7 and 8, we see that both storage modulus (G') and loss modulus (G'') increase with the electric field strength and the particle concentration over the entire strain range.

G', i.e. in-phase stress component with the strain, is observed to be larger than G'', i.e. the out-of-phase stress component, and these values were independent of the strain in the linear viscoelastic region. As we increased the applied strain, G'' became larger than G', and these moduli sharply decreased. This can be explained in terms of the elasticity of the ER fluid, which is generated by particle chain structures under an imposed electric field. Similar behavior has been

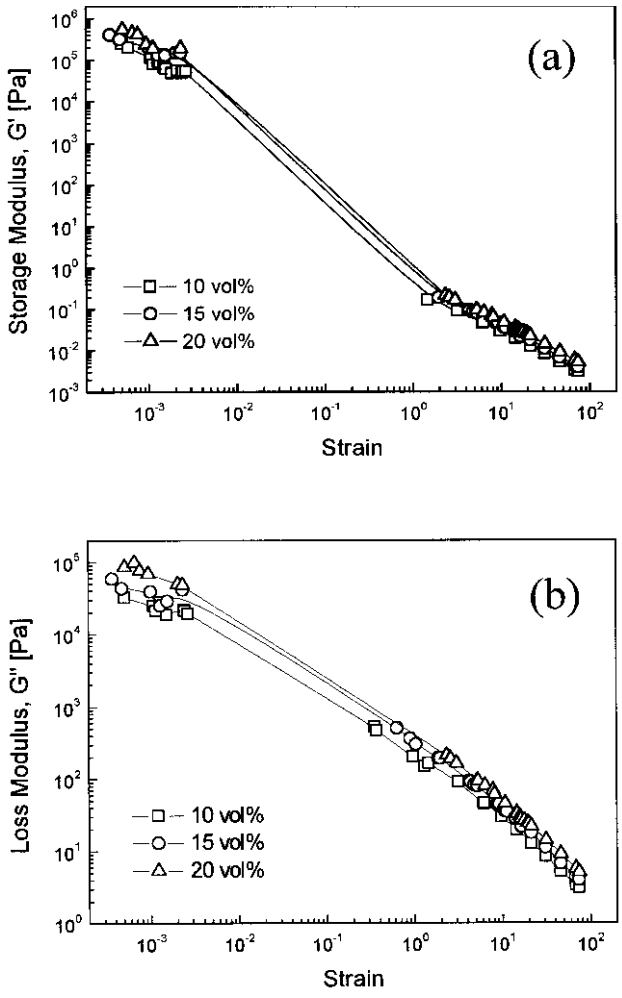

Fig. 8. (a) G' and (b) G'' as a function of strain amplitude for phosphate cellulose in silicone oil at three different particle concentrations, an electric field strength of 2 kV/mm and a frequency of 1 Hz.

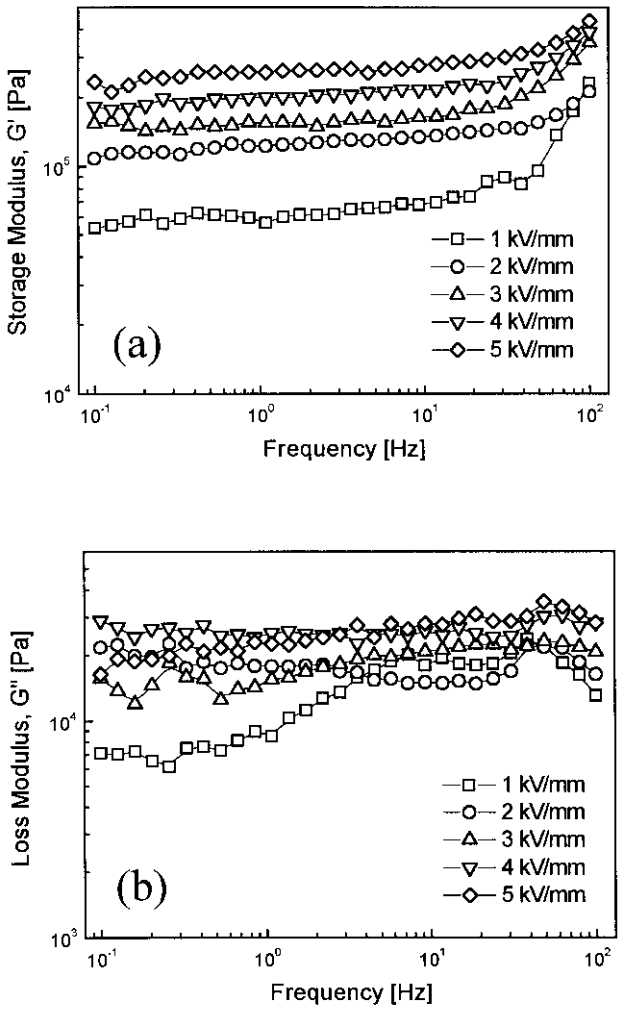

Fig. 9. (a) G' and (b) G'' as function of frequency for 20 vol% phosphate cellulose in silicone oil at five different electric field strengths and a strain of 0.002.

also observed for a corn starch in polybutene/kerosene ER fluid via a vertical oscillation rheometer [47,48]. When the fibrillar structures of the suspended phosphate cellulose particle sustain the applied strain, the elasticity is dominant in the linear viscoelastic region. However, as the strain is increased, the deformation begins to alter the structure; the structure breaks down beyond a certain degree of deformation, and finally the elasticity of the ER fluid disappeared abruptly.

Martin et al. [49] reported that they could not observe any linear viscoelastic region and claimed that the energy of the ER fluid was stored in G'. Compared to our results, however, it seems that their strain amplitude sweep began at 0.01, which is believed to be too large to find the linear viscoelastic region.

As shown in Figs. 7 and 8, G' remained constant and then decreased as the strain amplitude increased. As both the electric field strength and the particle concentration increased, the linear viscoelastic region became wider and the magnitude of both G' and G'' increased. The particle–particle interactions due to polarization contribute to the enhancement of the dynamic moduli and the steady shear viscosity to a great extent. The polarization forces between the particles increase with increasing both the electric field strength and the particle concentration, which in turn increases the particle chain length and the magnitude of G' and G''.

Figs. 9 and 10 show, respectively, the plots of G' and G'' as a function of the frequency with a small strain (0.002) in the linear viscoelastic region. It is shown that G' and G'' are either constant or increase slightly as the deformation frequency is increased to 10 Hz. At a high frequency range, G' increased slightly. This dependence is indicative of the relaxation modes existing in the frequency range examined. In relation to this point, it should be noted that the ω dependencies of G' and G'' are mutually related with each other through the Kramers–Krönig relationship [50]. The general shape of the G'' curves was similar, but the values fluctuated over a broad range of ω. It was observed that G'' showed a more sensitive dependence to the

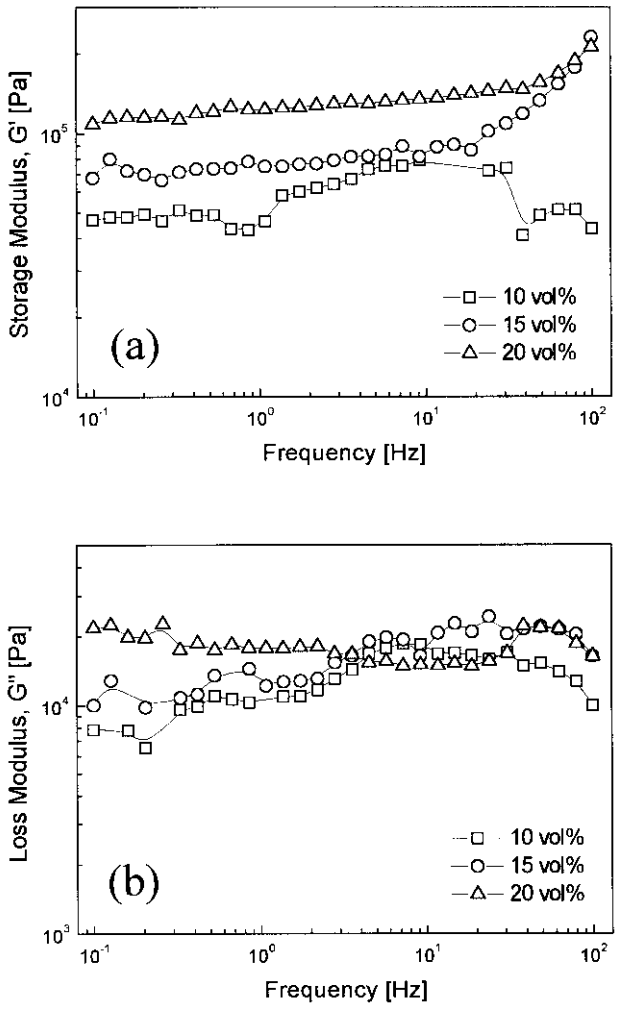

Fig. 10. (a) G' and (b) G'' as function of frequency for phosphate cellulose in silicone oil at three different particle concentrations, an electric field strength of 2 kV/mm and a strain of 0.002.

frequency sweep than G'. However, the magnitude of G' is somewhat larger than that of G'', and G' was more affected by the electric field strength and particle concentration than G''.

This is similar to the typical behavior of cross-linked rubbers [51], which do not relax in a given range of strain frequency. Because the relaxation of the internal chain structures of ER fluids was very slow, they exhibited the rubber-like behavior in the linear region. The increase in G' with both the applied electric field strength and particle concentration indicate that the ER fluid becomes more elastic with the electric fields under the linear viscoelastic conditions.

4. Conclusions

In this paper, phosphate cellulose particles were synthesized via a phosphate ester reaction between cellulose particles and a phosphoric acid–urea mixture. The ER properties of the phosphate cellulose/silicone oil suspension were then investigated by examining the effects of electric field strength and particle concentration on yield stress and G' and G''. Both the dynamic and static yield stress increased with both the electric field strength and the particle concentration. Furthermore, this ER fluid exhibited typical viscoelastic properties under an imposed electric field due to chain formation, and elasticity increased with the increase in both electric field strength and particle concentration.

Acknowledgements

This study was supported by grant from the KOSEF through Applied Rheology Center at Korean University, Korea. The authors also wish to thank the referees for their valuable comments.

References

[1] Tao R, Sun JM. Phys Rev Lett 1991;67:398.
[2] Sakurai R, See H, Saito T, Asai S, Sumita M. Rheol Acta 1999;38:478.
[3] Hao T, Xu Y. Int J Mod Phys B 1996;10:2885.
[4] Hao T, Kawai A, Ikazaki F. Int J Mod Phys B 1999;13:1758.
[5] Cho MS, Choi HJ, Chin IJ, Ahn WS. Microporous Mesoporous Mater 1999;32:233.
[6] Böse H. Int J Mod Phys B 1999;13:1878.
[7] Wen W, Tam WY, Sheng P. J Mater Sci Lett 1998;17:419.
[8] Choi HJ, Kim JW, Yoon SH, Fujiura R, Komatsu M, Jhon MS. J Mater Sci Lett 1999;18:1445.
[9] Block H, Kelly JP, Qin A, Watson T. Langmuir 1990;6:6.
[10] Choi HJ, Cho MS, Jhon MS. Int J Mod Phys B 1999;13:1901.
[11] Choi HJ, Kim TW, Cho MS, Kim SG, Jhon MS. Eur Polym J 1997;33:699.
[12] Lee JH, Cho MS, Choi HJ, Jhon MS. Colloid Polym Sci 1999;277:73.
[13] Quadrat O, Stejskal J, Kratochvíl P, Klason C, McQueen D, Kubát J, Sáha P. Synth Met 1998;97:37.
[14] Choi HJ, Lee JH, Cho MS, Jhon MS. Polym Engng Sci 1999;39:493.
[15] Cho MS, Kim TW, Choi HJ, Jhon MS. J Mater Sci Lett 1997;16:672.
[16] Cho MS, Choi HJ, To K. Macromol Rapid Commun 1998;19:271.
[17] Choi HJ, Kim JW, To K. Synth Met 1999;101:697.
[18] Trlica J, Sáha P, Quadrat O, Stejskal J. Physica A 2000;283:337.
[19] Bloodworth R, Wendt E. Int J Mod Phys B 1996;10:2951.
[20] Choi HJ, Kim JW, Noh MH, Lee DC, Jhon MS. J Mater Sci Lett 1999;18:1505.
[21] Kim JW, Choi HJ, Jhon MS. Macromol Symp 2000;155:229.
[22] Kim JW, Kim SG, Choi HJ, Jhon MS. Macromol Rapid Commun 1999;20:450.
[23] Kim BH, Jung JH, Joo J, Kim JW, Choi HJ. J Korean Phys Soc 2000;36:366.
[24] Heinze T. Macromol Chem Phys 1998;199:2341.
[25] Kawai A, Uchida K, Kamiya K, Gotoh A, Yoda S, Urabe F, Ikazaki F. Int J Mod Phys B 1996;10:2849.
[26] Ikazaki F, Kawai A, Uchida K, Kawakami T, Sakurai K, Anzai H, Asako Y. J Phys D: Appl Phys 1998;31:336.
[27] Ahn BG, Choi US, Kwon OK. Polym J 1999;31:494.
[28] Kim SG, Choi HJ, Jhon MS. Macromol Chem Phys 2000 (in press).
[29] Kim SG, Kim JW, Choi HJ, Suh MS, Shin MJ, Jhon MS. Colloid Polym Sci 2000;278:894.
[30] Arslanov SS, Rakhmanberdiev GR, Mirkamilov TM, Abidova F. Russ J Appl Chem 1995;68:444.
[31] Oka S. In: Eirich FR, editor. Rheology: theory and applications, vol. 3. New York: Academic Press, 1960. p. 33.

[32] Jhon MS, Kwon TM, Choi HJ, Karis TE. Ind Engng Chem Res 1996;35:3027.
[33] Kwon TM, Jhon MS, Choi HJ. J Mol Liq 1998;75:115.
[34] Choi HJ, Kwon TM, Jhon MS. J Mater Sci 2000;35:889.
[35] Aubry T, Largenton B, Moon M. Langmuir 1999;15:2380.
[36] Choi HJ, Cho MS, To K. Physica A 1998;254:272.
[37] Dealy JM, Wissburn KF. Melt rheology and its role in plastics processing: theory and applications. New York: Van Nostrand Reinhold, 1990. p. 18.
[38] Parthasarathy M, Klingenberg DJ. Mater Sci Engng 1996;R17:57.
[39] Halsey TC. Science 1992;258:761.
[40] Choi HJ, Cho MS, Kang KK, Ahn WS. Microporous Mesoporous Mater 2000;39:19.
[41] Cho MS, Kim JW, Choi HJ, Webber RM, Jhon MS. Colloid Polym Sci 2000;278:61.
[42] Block H, Kelly JP. J Phys D: Appl Phys 1988;21:1661.
[43] Klass DL, Martinek TW. J Appl Phys 1967;38:67.
[44] Klingenberg DJ, Van Swol F, Zukoski CF. J Chem Phys 1991;94:6170.
[45] Davis LC. J Appl Phys 1997;81:1985.
[46] Ginder JM, Davis LC, Lee LD. Int J Mod Phys B 1996;10:3293.
[47] Cho MS, Choi YJ, Choi HJ, Kim SG, Jhon MS. J Mol Liq 1998;75:13.
[48] Kim SG, Kim JW, Cho MS, Choi HJ, Jhon MS. J Appl Polym Sci 2001;79:108.
[49] Martin JE, Adolf D, Halsey TC. J Colloid Interface Sci 1994;167:437.
[50] Scaife BKP. Principles of dielectrics. Oxford: Clarendon Press, 1987. p. 55.
[51] Ferry JD. Viscoelastic properties of polymers. New York: Wiley, 1980. p. 33.